



Published in final edited form as:

Arthritis Rheumatol. 2022 September ; 74(9): 1524–1534. doi:10.1002/art.42124.

Peripheral $\gamma\delta$ T cells regulate neutrophil expansion and recruitment in experimental psoriatic arthritis

Cuong Thach Nguyen, PhD¹, Hiroki Furuya, MD, PhD², Dayasagar Das, PhD¹, Alina I Marusina, PhD³, Alexander A Merleev, PhD³, Resmi Ravindran, PhD⁴, Zahra Jalali, MD², Imran H. Khan, PhD⁴, Emanuel Maverakis, MD³, Iannis E. Adamopoulos, DPhil^{1,2,*}

¹Division of Rheumatology, Allergy and Clinical Immunology, University of California at Davis

²Department of Rheumatology, Beth Israel Deaconess Medical Center, Harvard Medical School, USA

³Department of Dermatology, University of California, Davis, Sacramento, CA, USA

⁴Department of Pathology and Laboratory Medicine, University of California at Davis, USA

Abstract

Objective: This study was undertaken to identify the mechanistic role of $\gamma\delta$ T cells in the pathogenesis of experimental psoriatic arthritis (PsA).

Methods: In this study, we perform IL-23 gene transfer in WT and TCR δ deficient mice and perform tissue phenotyping in the joint, skin, and nails to characterize the inflammatory infiltrate. We further perform detailed flow cytometry, immunofluorescence, RNAseq, T cell repertoire analysis and *in vitro* T-cell polarization assays to identify regulatory mechanisms of $\gamma\delta$ T cells.

Results: We demonstrate that $\gamma\delta$ T cells support systemic granulopoiesis which is critical for murine PsA-like pathology. Briefly, $\gamma\delta$ T cell ablation inhibited the expression of neutrophil chemokines CXCL-1, CXCL-2 and neutrophil CD11b⁺Ly6G⁺ accumulation in the aforementioned PsA-related tissues. Although a significantly reduced expression of GM-CSF and IL-17A was detected systemically in TCR $\delta^{-/-}$ mice, no GM-CSF⁺/IL-17A⁺ $\gamma\delta$ T cells were detected locally in the inflamed skin and/or bone marrow in WT mice. Our data demonstrate that non-resident $\gamma\delta$ T cells regulate the expansion of an CD11b⁺Ly6G⁺ neutrophil population and their recruitment to joint and skin tissues, where they develop hallmark pathologic features of human PsA.

***Correspondence:** Iannis E. Adamopoulos, Division of Rheumatology, and Clinical Immunology, Harvard Medical School, Beth Israel Medical Deaconess Center, Boston, MA. Tel 617-735-4162. iadamopo@bidmc.harvard.edu.

Author Contributions

All authors were involved in drafting the article or revising it critically for important intellectual content, and all authors approved the final version to be submitted for publication. Dr. Adamopoulos had full access to all of the data in the study and take responsibility for the integrity of the data and the accuracy of the data analysis.

Study conception and design: IE Adamopoulos

Acquisition of data: CT. Nguyen, H. Furuya, Daysagar Das, R Ravindran, A Marusina, A Merleev, Z. Jalali, IE Adamopoulos

Analysis and interpretation of data: CT. Nguyen, H. Furuya, I Khan, E Maverakis, Z. Jalali, IE Adamopoulos.

Disclosures

The authors have no financial conflicts of interest.

Conclusion: Our findings do not support that tissue-resident $\gamma\delta$ T cells are initiating the disease but demonstrate a novel role of $\gamma\delta$ T cells in neutrophil regulation that can be exploited therapeutically in PsA patients.

INTRODUCTION

Psoriatic arthritis (PsA) is a chronic, inflammatory, and heterogeneous disease that affects distinct anatomical sites including peripheral and axial joints, resulting in synovitis, enthesitis, onycholysis and epidermal hyperplasia (1). The cutaneous features of PsA are characterized by the accumulation of prominent neutrophilic exudates (Munro's microabscesses) and mixed dermal infiltrates including $\alpha\beta$ and $\gamma\delta$ T cells (2). Similarly, nail psoriasis and onycholysis is commonly associated with increased neutrophil populations in the affected nail bed (3) and clinically the neutrophil to lymphocyte ratio is a strong predictor for PsA(4).

Interleukin 23 (*IL23*) induces the differentiation, survival, and expansion of Th17, $\gamma\delta$ T cells and neutrophils (5, 6) and is also associated with PsA susceptibility and pathogenesis (7, 8). Although the exact mechanisms are not completely understood the activation of IL-17A producing $\gamma\delta$ T cells has been suggested. Activated $\gamma\delta$ T cells regulate multiple immune responses by producing pro-inflammatory cytokines including IL-17A, interferon- γ (IFN- γ) and tumor necrosis factor (TNF), and chemokines including C-C motif ligand 5 (CCL5), CXCL10, and lymphotactin (XCL1) which lead to the recruitment of neutrophils and macrophages (9). Additionally, $\gamma\delta$ T cells regulate myelopoiesis and activation of polymorphonuclear neutrophils through G-CSF, GM-CSF and M-CSF (10, 11) and absence of $\gamma\delta$ T cells prevents neutrophil accumulation in cancer (12). The contribution of these pathways in the pathogenesis of spondyloarthritis is of paramount importance as IL-17A⁺ $\gamma\delta$ T cells and double producing IL-17A⁺ GM-CSF⁺ $\gamma\delta$ T cells have been identified in spondyloarthritis patients (13, 14). Despite the high clinical significance and the fact that clinical trials of GM-CSF in spondyloarthritis are currently under way the cellular and molecular mechanisms of pathogenic $\gamma\delta$ T cells remain elusive.

In mice, the importance of $\gamma\delta$ T cells has been widely documented in experimental models of arthritis (15–17), and imiquimod-induced psoriasis (18, 19). $\gamma\delta$ T cells are also detected in inflamed skin and the entheses which are commonly observed in PsA patients, however as enthesitis can occur in the absence of $\gamma\delta$ T cells the functional evidence are weak (20, 21) as recently reviewed (22). The major discrepancies around $\gamma\delta$ T cell functionality stems out from the fact that different $\gamma\delta$ subtypes exist in different tissues, and regulate both pro- and anti-inflammatory responses based on the expression of cytokines and activation status. The fundamental subtype differences between human and murine $\gamma\delta$ T cells, and the suboptimal tools used in $\gamma\delta$ T cell research further confounded the results (22, 23).

In the current study, we performed IL-23 gene transfer in WT and TCR $\delta^{-/-}$ mice (which lack $\gamma\delta$ T cells) (24) that were purposely backcrossed in the B10.RIII mouse strain, (susceptible to autoimmunity), and report the functional role of $\gamma\delta$ T cells. A systemic rather than a local inflammation is the driver of the disease which is regulated by GM-CSF and IL-17A, and by chemotactic factors that are responsible for the accumulation of neutrophil exudates in

IL-23-induced synovitis, onycholysis, and epidermal hyperplasia, associated with PsA. Our data reconcile previous conflicting observations and demonstrate a novel role of $\gamma\delta$ T cells in neutrophil recruitment and inflammation at anatomical sites critical for the pathogenesis of psoriatic arthritis.

MATERIALS AND METHODS

Animals

B10.RIII and TCR $\delta^{-/-}$ C57BL/6 mice were purchased from Jackson Laboratories (Sacramento, CA). In order to generate TCR $\delta^{-/-}$ B10.RIII mice, TCR $\delta^{-/-}$ C57BL/6 mice were crossed with inbred B10.RIII mice over more than ten generations. Sex- and age-matched mice (8–12 weeks) were used for all experiments under specific pathogen-free conditions. All animal protocols were approved by Institutional Animal Care and Use Committee, Beth Israel Medical Deaconess Center.

Reagents

Monoclonal antibodies of anti-Ly6G (1A8) and anti- $\gamma\delta$ TCR (GL3) were purchased from R&D Systems (Minneapolis, MN) anti-CD11b (M1/70) from ebioscience and anti-IL-17A (TC11-18H10.1), anti-GM-CSF (MP1–22E9) and CD3e (145-2C11) from BioLegend (USA). IRDye® 680CW goat anti-mouse/anti-rabbit secondary antibodies were purchased from LI-COR Biosciences (Lincoln, NE). IL-23 and IL-27p28 ELISA kits were purchased from eBioscience and R&D Systems respectively. EndoFree Plasmid Mega Kit was purchased from Qiagen, and Bio-Plex Pro™ mouse cytokine 23-plex assays was purchased from Bio-Rad. Minicircle-RSV.Flag.mIL23.elasti.bpA or RSV.eGFP.bpA (IL-23MC) was produced as previously described and injected hydrodynamically via tail vein delivery (25). Serum evaluation of IL-23 and clinical score was performed as previously described (25).

Flow cytometry

Bone marrow (BM) cells were isolated from B10.RIII mice 2 days post gene transfer of either GFP or IL-23MC. BM cells were flushed out using a 27-gauge needle attached to a 1 ml syringe containing PBS. Red blood cells were lysed with BD Pharm Lyse (BD Biosciences). Non-specific binding was blocked with TruStain FcX antibody (BioLegend) for 10 min at 4 °C in FACS buffer (Ca²⁺/Mg²⁺-free PBS with 2% FBS and 0.5 M EDTA) before staining (30 min) with appropriate antibodies. Isotype controls were used at the same protein concentrations as their corresponding markers. AccuCheck counting beads (Life Technologies) or Precision Count Beads (BioLegend) were used to determine absolute cell number per cm² based on the manufacturer's protocol. Flow cytometry was performed on BD FACSAria flow cytometer (BD Biosciences) or Attune Cytometer (Life Technologies) and the data was analyzed using FlowJo software (Tree Star, Ashland, OR, USA).

RNA isolation and Real-time PCR

RNA was isolated from mouse tissues using the RNeasy kit (Qiagen) including a DNase I digest step. Quality of RNA was analyzed with a Nanodrop spectrophotometer (Thermo Fisher Scientific). cDNA was prepared using iScript cDNA Synthesis Kit (Bio-Rad, Hercules, CA). qRT-PCR was performed using iTaq Universal SYBR Green Supermix

(Bio-Rad, Hercules, CA) according to the manufacturer's instructions. Relative expression of target genes was performed using the 2^{-CT} method and normalized with internal GAPDH control as previously described (25).

H&E and Immunohistochemistry

Murine ears, paws, and nails (decalcified in 15% ethylenediaminetetraacetic acid) were fixed in 10% formalin in PBS and paraffin embedded for sectioning (6 μ m). Tissue sections were stained with hematoxylin and eosin Y (Sigma). Photos were visualized and analyzed by Olympus BX61 microscope and BZ-II Analyzer software. Analysis and quantification were performed using ImageJ software. Histology sections (6 μ m) of each paraffin block were stained used for immunofluorescence microscopy as previously described (26). Sections were deparaffinized and blocked for 1 hour in blocking buffer (1% triton X, 2% BSA), then immunostained with appropriate antibodies and DAPI before visualized using a confocal microscope (Nikon C1). Quantification of neutrophils in the nail bed and synovium and bone resorption area was done using the point-counting method by using a counting grid overlaid over x400 magnification as previously described (27).

$\gamma\delta$ T cell expansion culture

$\gamma\delta$ T cell were cultured as previously described (28). Briefly, splenocyte were cultured at 1×10^6 cells per ml in RPMI 1640 containing 10% FCS, antibiotics, 1 X Glutamax (Gibco), 10mM HEPES (Gibco), 1mM sodium pyruvate (Gibco), 55 μ M β -mercaptoethanol and non-essential amino acids (Gibco) with 5ng/ml recombinant IL-23 (R&D Systems), 5ng/ml rIL-1 β (R&D Systems) and 10 μ g/ml anti-IFN-g (BioLegend) in 96-well round-bottom plates coated with 1 μ g/ml anti-TCR- $\gamma\delta$ (clone GL3; Biolegend) for 3 days. Cells were washed and re-seeded on fresh plastic at 1×10^6 cells/ml for a further 3 days as above without TCR- $\gamma\delta$ stimulation. Cells were collected at day 6 for flow cytometry analysis.

RNA seq

RNA was isolated from murine ears of WT or TCR $\delta^{-/-}$ mice injected with GFP MC either IL-23 MC using RNeasy Plus mini kit (Qiagen) and analyzed with Bioanalyzer. Purified total RNA (RIN value >5) was used for library preparation. The 3' Tag RNA-Seq run was performed on an Illumina HiSeq 4000 and generated an average of 600,000 reads per sample. RNA-Seq reads for the 9 individual samples including three groups: control (WT+GFP MC), treatment (WT+IL-23 MC), and mutant (TCR $\delta^{-/-}$ +IL-23 MC) and three replicates each, barcoded and run on a single lane) were independently aligned to the mouse genome (ref. ID: GRCh38.p6) using the STAR v2.7.0a alignment software with the corresponding ensembl reference genome. The featureCounts package was used to count the mapped reads and the edgeR package was used for differential expression analysis. Names of differentially expressed genes that meets criteria 1) fold change more than 2 and 2) FDR less than 0.05 are collected and used for further gene enrichment analysis. Enrichment analysis was performed using web-based tool "Enrichr" (29).

T cell repertoire analysis

Mouse ears (9 mice/group) were stabilized by addition of RNAlater (Ambion) and homogenized using TissueLyzer II (Qiagen). Total RNA was extracted using the RNeasy Fibrosis mini kit (Qiagen) and quantified using a Qubit Fluorometer. RNA integrity was assessed using the *RNA* ScreenTape on Agilent TapeStation (Agilent), with RIN (RNA integrity number) ≥ 8 set as an inclusion cutoff. Indexed libraries were constructed from 2000 ng of total RNA using the TruSeq Stranded mRNA Sample Prep Kit (Illumina) following the manufacturer's instruction. The quantity and quality of the libraries were also assessed by Qubit and D1000 ScreenTape on Agilent TapeStation (Agilent), respectively. To maximize CDR3 reads, the average library size was 400 bp. The libraries' molar concentration was validated by qPCR for library pooling. Sequencing was performed on the Illumina HiSeq 4000 platform using PE150 chemistry (Illumina).

Data availability

RNA-seq data was deposited in the NCBI Sequence Read Archive under accession number SUB10952655 (Temporary Submission ID).

Statistical analysis

Statistical differences were analyzed by Mann–Whitney test. All results are representative of at least 3 independent experiments, unless otherwise stated. Statistically significant differences were considered as $P < 0.05$ (* $P < 0.05$, ** $P < 0.01$, *** $P < 0.001$). Data represent mean \pm SEM (standard error of the mean) of three independent experiments.

RESULTS

$\gamma\delta$ T cell deficiency limits IL-23-induced joint inflammation

To examine the role of $\gamma\delta$ T cells in joint inflammation, we performed IL-23 gene transfer in WT and TCR $\delta^{-/-}$ mice using hydrodynamic gene delivery of minicircle IL-23 as previously described (Fig. 1A–B) (25). IL-23 gene transfer induced swelling and paw erythema of murine paws accompanied by synovial inflammation (Fig. 1C–E), which was absent in control mice. TCR $\delta^{-/-}$ mice showed significant decrease of disease severity (WT: $8.8 \pm 2.9\%$ vs TCR $\delta^{-/-}$: $2.5 \pm 1.3\%$, $p < 0.05$) and disease incidence (WT: $86.0 \pm 12.8\%$ vs TCR $\delta^{-/-}$: $43.6 \pm 14.4\%$, $p < 0.01$) compared to WT mice at day 10 post IL-23 MC gene transfer (Fig. 1C–E). H&E stain of ankle joints 11 days post IL-23 gene transfer showed that WT mice had a hyperplastic and inflamed synovium with a mixed inflammatory infiltrate of mononuclear cells and numerous polymorphonuclear leukocytes, and evidence of bone destruction (Fig. 1F & Supplementary Fig 1), consistent with previous observations (25, 30). The enthesis maintained normal architecture in both enthesis fibrous part and fibrocartilage tissue adjacent to the bone region. The corresponding tendon sheaths revealed slight inflammation accompanied by no or minimal edema, altered vascularity and disorganized collagen fibers. No collagen hyalinization was found in the extracellular matrix. The bone-tendon borders were minimally blurred, though, without any appreciable irregularity or focal defect at the interface of the fibrous attachment to the periosteum. In the absence of extensive infiltration of enthesis, widely dispersed inflammatory infiltrates in the muscle

were evident suggestive of mild myositis and tendinitis. Flow cytometric analysis 48 hours post-IL-23 gene transfer confirmed an increase in CD11b⁺Ly6G⁺ cells (GFP MC: 12.90 ± 0.74%, IL-23 MC: 23.87 ± 1.87%, $p < 0.01$) in the bone marrow of WT mice (Figure 1G). This pathology was accompanied by a marked elevation of gene expression of synovial inflammatory markers *Il-1 β* , *Vcam-1* (vascular cell adhesion molecule 1), *Mpp3* (matrix metalloproteinase 3), *Pecam-1* (platelet and endothelial cell adhesion molecule-1) as well as osteoclast related markers *Tnfrsf11a* (RANK, Receptor activator of nuclear factor K Beta), *Ctsk* (Cathepsin K), and *Acp5* (Tartrate resistant acid phosphatase) (Fig. 1H). Collectively, our data confirmed that genetic ablation of $\gamma\delta$ T cells reduces joint inflammation and neutrophil expansion.

$\gamma\delta$ T cell deficiency prevents neutrophil accumulation in PsA related tissues

IL-23 gene transfer also resulted in severe inflammation with psoriatic lesions of the distal nail bed and hyponychium, and in severe cases resulted in onycholysis (Fig. 2A) which is commonly observed in PsA patients. The inflammatory infiltrate of the nail bed consisted largely of polymorphonuclear neutrophils similar to the bone marrow. This was confirmed by immunofluorescent staining using neutrophil specific antibodies (anti-Ly6G). TCR $\delta^{-/-}$ mice were protected from IL-23-induced nail psoriasis and onycholysis, and this correlated with a decrease of neutrophil accumulation in the nail bed (Fig. 2B, Supplementary Fig 1). To investigate whether $\gamma\delta$ T cells modulate activation of neutrophil during joint and skin inflammation, neutrophil markers were examined by qRT-PCR in paws and ear tissue, respectively. Our results showed that IL-23 increased expression of neutrophil markers in joint and skin and TCR $\delta^{-/-}$ mice differentially regulated the neutrophil marker expression in these tissues. Specifically, IL-23-induced expression of *Cd11b*, *Mpo*, *Cxcr2*, and *Frp1* was prevented within the joint (Fig. 2C) and *Cd11b* and *Cxcr2* induction was prevented in the skin (Fig 2D). Collectively, these results indicate that neutrophilic inflammation in nail, skin, joint are down-regulated in TCR $\delta^{-/-}$ mice.

$\gamma\delta$ T cell deficiency suppresses IL-23-induced innate skin inflammation.

To investigate whether $\gamma\delta$ T cells are required for the IL-23-induced skin inflammation, we examined parameters of skin inflammation between WT and TCR $\delta^{-/-}$ mice. IL-23 induced erythema with silvery white scales at 11 days post IL-23 gene transfer (Fig. 3A) in WT mice but not in TCR $\delta^{-/-}$ mice. The clinical observation was corroborated by histological analysis which demonstrated limited thickening of the epidermis, infiltration by inflammatory cells, and formation of neutrophilic exudates (Munro's microabscesses) in TCR $\delta^{-/-}$ compared to WT mice (Fig. 3B–D & Supplementary Fig 1). Immunofluorescence imaging of ears with neutrophil specific antibodies after IL-23 gene transfer confirmed that neutrophils accumulate in the skin in WT mice compared to mice injected with control GFP MC and TCR $\delta^{-/-}$ mice (Fig. 3E). Furthermore, IL-23 gene transfer in WT mice showed a significant increased expression of inflammatory gene markers *K16*, *S100a7*, *S100a8*, *S100a9*, *Cxcl1*, *Cxcl2*, *Il23r*, *Il17*, *Il22*, and *Il6*, compared to TCR $\delta^{-/-}$ mice (Fig. 3F). Collectively, skin inflammation showed an increase in neutrophil accumulation and neutrophil chemokines that was prevented in TCR $\delta^{-/-}$ mice.

IL-23-induced skin inflammation is not associated with expansion of dermal $\gamma\delta$ T cells.

To investigate mechanistically the role of $\gamma\delta$ T cells in IL-23-induced skin inflammation, we performed RNA-Seq on ear tissue collected from WT and TCR $\delta^{-/-}$ mice 11 days post GFP and/or IL-23 gene transfer. This analysis identified 2,800 genes that were meaningfully (fold change >2) and significantly (FDR > 2) differentially expressed in WT animals following IL-23MC compared to GFP MC controls. Among the 30 most variable genes (Figure 4A) several genes classically associated with psoriasis including *Krt16*, *S100a8*, *S100a9* (FC = 752, 1562, and 1741, respectively; $p = 2.37\text{e-}05$, $3.85\text{e-}06$, and $3.41\text{e-}06$, respectively) were significantly increased. The expression of several neutrophil-attracting chemokines was also upregulated including *Cxcl2* and *Cxcl5* as well as the T cell and monocyte-attracting chemokine *Cxcl10* (FC = 1415, 3.96, and 41.74 respectively and $p = 5.73\text{e-}04$, $9.89\text{e-}04$, and $3.79\text{e-}02$, respectively). Other genes of interest included neutrophil proteases and genes associated with neutrophil activation, including innate pro-inflammatory mediators such as *Il1 β* and *Ptgs2* (FC = 1125 and 182, respectively; $p = 5.85\text{e-}04$ and $2.36\text{e-}02$, respectively) (Fig. 4A & Supplementary Figure 2). Hierarchical clustering heatmap of differentially expressed genes (DEG's) revealed that TCR $\delta^{-/-}$ mice show greater similarity to WT GFP control mice, than to IL-23 minicircle treated mice (Fig. 4A). Accordingly, Gene Ontology analyses of the upregulated genes in IL-23 gene transferred WT mice showed multiple terms that was compatible with psoriasis, such as "Inflammatory response", "Keratinization", "Neutrophil chemotaxis" and "Neutrophil migration" (Fig. 4B). To characterize the IL-23 gene transfer induced alterations in the T cell repertoire, TCR gene segments and the TCR complementarity determining region 3 (CDR3)-encoding sequences were mined from RNA-Seq datasets of WT GFP MC and IL-23 MC mice. Surprisingly, IL-23 induced a significant decrease of $\gamma\delta$ T cells in the skin (Supplementary Figure 3). Specifically, the dominant TRD clone (CGSDIGGSSWDTRQMFF), which normally comprised 70% of the TRD repertoire, declined to 53% and the second most dominant clone in the TRD repertoire (CALYRRDATDKLVF) dropped to below detection in the skin following IL-23 gene transfer (Fig. 4C). Consistent with these findings flow cytometry after GFP/IL-23 gene transfer revealed no significant increase in absolute number of $\gamma\delta$ T cells count or proportion of GM-CSF/IL-17 producing $\gamma\delta$ T cells among $\gamma\delta$ T cells (Figure 4D–E); not even in mRNA levels (Figure 4F). We also performed similar analysis at the bone marrow and again no $\gamma\delta$ T cell expansion was observed (Supplementary Figure 4).

IL-23 induces the development of IL-17A⁺/GM-CSF⁺ $\gamma\delta$ T cells *in vitro*.

Despite the absence of IL-17A/GM-CSF double positive of $\gamma\delta$ T cells in the skin and bone marrow, the levels of pro-inflammatory cytokines including GM-CSF and other myeloid supporting factors were decreased in the circulation in the TCR $\delta^{-/-}$ mice (Figure 5A and Supplementary Figure 5). To confirm that indeed $\gamma\delta$ T cells express GM-CSF, we performed experiments to determine the requirements of IL-17A⁺/GM-CSF⁺ $\gamma\delta$ T cells differentiation *in vitro* using cytokines and antigen activation (Figure 5B). Our data showed that IL-23, IL-1 β , anti-IFN γ and anti- TCR δ antibodies resulted in the differentiation of IL-17A/GM-CSF double positive cells in splenocyte cultures isolated from WT mice (Figure 5C–D and Supplementary Figure 6). These experiments also confirmed that the IL-17A/GM-CSF double positive cells were mainly (95%) $\gamma\delta$ T cells (Figure 5D–F). Collectively our data demonstrate that although IL-23 can induce the development of IL-17A⁺/GM-CSF⁺ $\gamma\delta$ T

cells, other factors are also required and therefore, a systemic elevation of IL-23 is not adequate to induce IL-17A⁺/GM-CSF⁺ $\gamma\delta$ T cells.

DISCUSSION

Here we demonstrate the importance of $\gamma\delta$ T cells in the development of PsA-like pathology at multiple anatomical sites by applying IL-23 gene transfer technology in mice lacking $\gamma\delta$ T cells. In our model IL-23 gene transfer in mice elicits skin and joint pathology reminiscent of PsA which is suppressed in mice lacking $\gamma\delta$ T cells. Other groups have also demonstrated that the absence of $\gamma\delta$ T cells prevented neutrophil accumulation and indicated the importance of the $\gamma\delta$ T cell/IL-17/neutrophil axis in metastatic disease and that $\gamma\delta$ T cells modulate myeloid cell recruitment during peripheral inflammation (12). Myeloid recruitment was also affected by genetic ablation of $\gamma\delta$ T cells in inflammatory pain models (31). However, our findings do not support a local role of resident $\gamma\delta$ T cells but rather role of $\gamma\delta$ T cells in modulating systemic neutrophil infiltration.

Specifically, we demonstrate that $\gamma\delta$ T cells regulate pro-inflammatory cytokines including GM-CSF, IL-6, IFN- γ , TNF, and neutrophil specific chemokines CXCL-1, and CXCL-2 in the circulation which limits myeloid expansion and neutrophil migration (32). The absence of neutrophil recruitment and the reduction in the inflammatory infiltrate in TCR δ ^{-/-} mice leads to a reduction of IL-17, (33) TNF, (34) and other pro-osteoclastogenic factors (35) and hence reduced bone resorption. Our data are in agreement with previous observations where depletion of neutrophil prevents joint inflammation (36). Similar to synovitis, $\gamma\delta$ T cells deficiency also inhibited IL-23-induced onycholysis, which was again accompanied by a reduced accumulation of Ly6G⁺ cell neutrophils in the nail bed. These data correlate well with the human disease where and neutrophilic abscess are commonly observed in nail bed epithelium of patients with nail psoriasis (37).

We focused more on the biology of the skin as at least in adult patients' psoriasis precedes joint inflammation. Therefore, we reasoned that skin inflammation may provide mechanistic clues of disease initiation and pathogenesis. The neutrophilic inflammation in the upper dermis was reminiscent to the pathologic features of human psoriasis and the formation of Munro's microabscesses and consistent with multiple studies that have shown the dependence of skin inflammation on neutrophils (26, 38). The reduction of neutrophil and inflammation in the skin despite the high levels of mRNA IL-17A locally in the skin suggest that IL-17A pathology is mediated by myelopoiesis and neutrophil migration rather than a local effect of IL-17A. This is in agreement with previous observations where IL-17A local injections failed to induce skin inflammation (39) and adoptive transfer of Ly6G⁺ cells was sufficient to induce skin pathology in the absence of exogenous IL-17A (26). Therefore, it is also not surprising that dermal IL-17A⁺ $\gamma\delta$ T cells did not expand in the skin following IL-23 gene transfer. In fact, this data are in agreement with previous observations where IL-23 gene transfer in the SKG mice only affected the number of $\gamma\delta$ T cells in the lymph nodes (40). Of course, as previously mentioned using the imiquimod animal model, which activates Toll-like receptors IL-17A⁺ $\gamma\delta$ T cells are commonly observed (18, 19) and we confirmed these observations with *in vitro* stimulations. Our key finding that $\gamma\delta$ T cells did not expand in the skin, was corroborated by T cell repertoire analysis. The marked reduction

(46%) of total clones and (17%) of the TCRD dominant clone in the IL-23 gene transfer compared to GFP control are also in agreement with data from other groups demonstrating the majority of T cells in psoriatic skin are expressing $\alpha\beta$ TCRs (41, 42). Notably, a systemic elevation of the anti-inflammatory cytokine IL-27 which is known to inhibit $\alpha\beta$ T cell development and osteoclastogenesis leading to bone loss was observed in TCR $^{\delta-/-}$ mice suggesting that local inflammation may be regulated remotely (30, 43, 44). This is also corroborated by the fact that IL-17A levels were reduced in the circulation in TCR $^{\delta-/-}$ mice.

One limitation of our study is that we did not detect where the IL-17A $^+$ $\gamma\delta$ T cells are expanded, and more sophisticated experiments with reporter mice would need to address that. However we postulate that tissues that are rich in $\gamma\delta$ T cell polarizing factors like the peritoneal cavity may be a suitable location for the development of IL-17A $^+$ GM-CSF $^+$ $\gamma\delta$ T cells in our model (45, 46). An additional point to consider is that $\gamma\delta$ T cells may regulate indirectly other GM-CSF producing cells such as NK cells (47) and collectively regulate myelopoiesis. Whatever the mechanism, direct or indirect we hereby demonstrate that $\gamma\delta$ T cells are required for IL-23-induced pathology and regulate neutrophil accumulation in the skin, spleen, bone marrow and the joints.

Neutrophils are also important effector cells in enthesal inflammation and the activation of neutrophils is critical in determining the development of enthesitis in man (48). In mice previous reports have suggested that in the IL-23 MC model CD3 $^+$ CD4 $^-$ CD8 $^-$ cells are critical in murine enthesitis (49) however other groups have demonstrated that enthesitis can occur in the absence of CD3 $^+$ CD4 $^-$ CD8 $^-$ $\alpha\beta$ and $\gamma\delta$ T cells (21, 50). Notably, a recent study failed to recapitulate the observations of IL-23-induced enthesitis using the IL-23MC model (51). Consistent with our original report in our seminal IL-23MC paper (52), we did not detect enthesitis. Our data confirm that the enthesitis is not inflamed at all in this model at the time-points tested and thus it cannot be responsible for disease pathogenesis (21, 50) (51).

The identification of double producing IL-17A $^+$ GM-CSF $^+$ $\gamma\delta$ T cells in the circulation of spondyloarthritis patients (13, 14) has already hinted to the importance of granulopoiesis and the systemic nature of SpA. The data presented herein support a model of PsA as a systemic disease and demonstrates a systemic modulatory role of $\gamma\delta$ T cells in IL-23-induced pathogenesis and provide a strong mechanistic rationale to support clinical trials that modulate myelopoiesis in PsA.

Supplementary Material

Refer to Web version on PubMed Central for supplementary material.

Financial support

This work was supported by National Institutes of Health/National Institute of Arthritis and Musculoskeletal and Skin Diseases Grant 2R01AR062173, and a National Psoriasis Foundation Translational Research grant to IEA.

Abbreviations used in this article

PsA Psoriatic arthritis

BM	Bone marrow
MC IL-23	minicircle IL-23
WT	wildtype
DEG	differentially expressed genes
CDR3	complementarity determining region 3
TRD	T cell receptor delta

References

1. Ritchlin CT, Colbert RA, Gladman DD. Psoriatic Arthritis. *N Engl J Med*. 2017;376(10):957–70. [PubMed: 28273019]
2. Nestle FO, Kaplan DH, Barker J. Psoriasis. *N Engl J Med*. 2009;361(5):496–509. [PubMed: 19641206]
3. Werner B, Fonseca GP, Seidel G. Microscopic nail clipping findings in patients with psoriasis. *Am J Dermatopathol*. 2015;37(6):429–39. [PubMed: 25993403]
4. Kim DS, Shin D, Lee MS, Kim HJ, Kim DY, Kim SM, et al. Assessments of neutrophil to lymphocyte ratio and platelet to lymphocyte ratio in Korean patients with psoriasis vulgaris and psoriatic arthritis. *J Dermatol*. 2016;43(3):305–10. [PubMed: 26381893]
5. Sutton CE, Lalor SJ, Sweeney CM, Brereton CF, Lavelle EC, Mills KH. Interleukin-1 and IL-23 induce innate IL-17 production from gammadelta T cells, amplifying Th17 responses and autoimmunity. *Immunity*. 2009;31(2):331–41. [PubMed: 19682929]
6. Smith E, Zarbock A, Stark MA, Burcin TL, Bruce AC, Foley P, et al. IL-23 is required for neutrophil homeostasis in normal and neutrophilic mice. *J Immunol*. 2007;179(12):8274–9. [PubMed: 18056371]
7. Filer C, Ho P, Smith RL, Griffiths C, Young HS, Worthington J, et al. Investigation of association of the IL12B and IL23R genes with psoriatic arthritis. *Arthritis and rheumatism*. 2008;58(12):3705–9. [PubMed: 19035472]
8. Bowes J, Orozco G, Flynn E, Ho P, Brier R, Marzo-Ortega H, et al. Confirmation of TNIP1 and IL23A as susceptibility loci for psoriatic arthritis. *Ann Rheum Dis*. 2011;70(9):1641–4. [PubMed: 21623003]
9. Vantourout P, Hayday A. Six-of-the-best: unique contributions of $\gamma\delta$ T cells to immunology. *Nat Rev Immunol*. 2013;13(2):88–100. [PubMed: 23348415]
10. Stark MA, Huo Y, Burcin TL, Morris MA, Olson TS, Ley K. Phagocytosis of apoptotic neutrophils regulates granulopoiesis via IL-23 and IL-17. *Immunity*. 2005;22(3):285–94. [PubMed: 15780986]
11. Mamedov MR, Scholzen A, Nair RV, Cumnock K, Kenkel JA, Oliveira JHM, et al. A Macrophage Colony-Stimulating-Factor-Producing $\gamma\delta$ T Cell Subset Prevents Malarial Parasitemic Recurrence. *Immunity*. 2018;48(2):350–63.e7. [PubMed: 29426701]
12. Coffelt SB, Kersten K, Doornebal CW, Weiden J, Vrijland K, Hau C-S, et al. IL-17-producing $\gamma\delta$ T cells and neutrophils conspire to promote breast cancer metastasis. *Nature*. 2015;522(7556):345–8. [PubMed: 25822788]
13. Venken K, Jacques P, Mortier C, Labadia ME, Decruy T, Coudensys J, et al. ROR γ t inhibition selectively targets IL-17 producing iNKT and $\gamma\delta$ -T cells enriched in Spondyloarthritis patients. *Nat Commun*. 2019;10(1):9. [PubMed: 30602780]
14. Al-Mossawi MH, Chen L, Fang H, Ridley A, de Wit J, Yager N, et al. Unique transcriptome signatures and GM-CSF expression in lymphocytes from patients with spondyloarthritis. *Nat Commun*. 2017;8(1):1510. [PubMed: 29142230]
15. Roark CL, French JD, Taylor MA, Bendele AM, Born WK, O'Brien RL. Exacerbation of collagen-induced arthritis by oligoclonal, IL-17-producing gamma delta T cells. *J Immunol*. 2007;179(8):5576–83. [PubMed: 17911645]

16. Ito Y, Usui T, Kobayashi S, Iguchi-Hashimoto M, Ito H, Yoshitomi H, et al. $\gamma\delta$ T cells are the predominant source of interleukin-17 in affected joints in collagen-induced arthritis, but not in rheumatoid arthritis. *Arthritis Rheum.* 2009;60(8):2294–303. [PubMed: 19644886]
17. Akitsu A, Ishigame H, Kakuta S, Chung S-H, Ikeda S, Shimizu K, et al. IL-1 receptor antagonist-deficient mice develop autoimmune arthritis due to intrinsic activation of IL-17-producing CCR2(+)V γ 6(+) $\gamma\delta$ T cells. *Nat Commun.* 2015;6:7464-. [PubMed: 26108163]
18. Pantelyushin S, Haak S, Ingold B, Kulig P, Heppner FL, Navarini AA, et al. Rorgammat+ innate lymphocytes and gammadelta T cells initiate psoriasiform plaque formation in mice. *The Journal of clinical investigation.* 2012;122(6):2252–6. [PubMed: 22546855]
19. Cai Y, Shen X, Ding C, Qi C, Li K, Li X, et al. Pivotal role of dermal IL-17-producing gammadelta T cells in skin inflammation. *Immunity.* 2011;35(4):596–610. [PubMed: 21982596]
20. Corthay A, Hansson AS, Holmdahl R. T lymphocytes are not required for the spontaneous development of enthesal ossification leading to marginal ankylosis in the DBA/1 mouse. *Arthritis Rheum.* 2000;43(4):844–51. [PubMed: 10765929]
21. Jacques P, Lambrecht S, Verheugen E, Pauwels E, Kollias G, Armaka M, et al. Proof of concept: enthesitis and new bone formation in spondyloarthritis are driven by mechanical strain and stromal cells. *Ann Rheum Dis.* 2014;73(2):437–45. [PubMed: 23921997]
22. Nguyen CT, Maverakis E, Eberl M, Adamopoulos IE. gammadelta T cells in rheumatic diseases: from fundamental mechanisms to autoimmunity. *Semin Immunopathol.* 2019;41(5):595–605. [PubMed: 31506867]
23. Koenecke C, Chennupati V, Schmitz S, Malissen B, Förster R, Prinz I. In vivo application of mAb directed against the $\gamma\delta$ TCR does not deplete but generates “invisible” $\gamma\delta$ T cells. *European Journal of Immunology.* 2009;39(2):372–9. [PubMed: 19130484]
24. Itohara S, Mombaerts P, Lafaille J, Iacomini J, Nelson A, Clarke AR, et al. T cell receptor delta gene mutant mice: independent generation of alpha beta T cells and programmed rearrangements of gamma delta TCR genes. *Cell.* 1993;72(3):337–48. [PubMed: 8381716]
25. Adamopoulos IE, Tessmer M, Chao C-C, Adda S, Gorman D, Petro M, et al. IL-23 is critical for induction of arthritis, osteoclast formation, and maintenance of bone mass. *J Immunol.* 2011;187(2):951–9. [PubMed: 21670317]
26. Suzuki E, Maverakis E, Sarin R, Bouchareychas L, Kuchroo VK, Nestle FO, et al. T Cell-Independent Mechanisms Associated with Neutrophil Extracellular Trap Formation and Selective Autophagy in IL-17A-Mediated Epidermal Hyperplasia. *J Immunol.* 2016;197(11):4403–12. [PubMed: 27798153]
27. Adamopoulos IE, Sabokbar A, Wordsworth BP, Carr A, Ferguson DJ, Athanasou NA. Synovial fluid macrophages are capable of osteoclast formation and resorption. *J Pathol.* 2006;208(1):35–43. [PubMed: 16278818]
28. McKenzie DR, Kara EE, Bastow CR, Tyllis TS, Fenix KA, Gregor CE, et al. IL-17-producing gammadelta T cells switch migratory patterns between resting and activated states. *Nat Commun.* 2017;8:15632. [PubMed: 28580944]
29. Chen EY, Tan CM, Kou Y, Duan Q, Wang Z, Meirelles GV, et al. Enrichr: interactive and collaborative HTML5 gene list enrichment analysis tool. *BMC Bioinformatics.* 2013;14:128. [PubMed: 23586463]
30. Bouchareychas L, Grossinger EM, Kang M, Adamopoulos IE. gammadeltaTCR regulates production of interleukin-27 by neutrophils and attenuates inflammatory arthritis. *Sci Rep.* 2018;8(1):7590. [PubMed: 29765156]
31. Petrovic J, Silva JR, Bannerman CA, Segal JP, Marshall AS, Haird CM, et al. gammadelta T Cells Modulate Myeloid Cell Recruitment but Not Pain During Peripheral Inflammation. *Front Immunol.* 2019;10:473. [PubMed: 30936874]
32. Griffin GK, Newton G, Tarrío ML, Bu D-x, Maganto-Garcia E, Azcutia V, et al. IL-17 and TNF- α sustain neutrophil recruitment during inflammation through synergistic effects on endothelial activation. *J Immunol.* 2012;188(12):6287–99. [PubMed: 22566565]
33. Adamopoulos IE, Chao C-C, Geissler R, Laface D, Blumenschein W, Iwakura Y, et al. Interleukin-17A upregulates receptor activator of NF- κ B on osteoclast precursors. *Arthritis Res Ther.* 2010;12(1):R29–R. [PubMed: 20167120]

34. Zhang Y-H, Heulsmann A, Tondravi MM, Mukherjee A, Abu-Amer Y. Tumor Necrosis Factor-alpha (TNF) Stimulates RANKL-induced Osteoclastogenesis via Coupling of TNF Type 1 Receptor and RANK Signaling Pathways. *J Biol Chem.* 2001;276(1):563–8. [PubMed: 11032840]
35. Adamopoulos IE, Mellins ED. Alternative pathways of osteoclastogenesis in inflammatory arthritis. *Nat Rev Rheumatol.* 2015;11(3):189–94. [PubMed: 25422000]
36. Wipke BT, Allen PM. Essential role of neutrophils in the initiation and progression of a murine model of rheumatoid arthritis. 2001. p. 1601–8.
37. Kaul S, Singal A, Grover C, Sharma S. Clinical and histological spectrum of nail psoriasis: A cross-sectional study. *J Cutan Pathol.* 2018;45(11):824–30. [PubMed: 30073694]
38. Schon M, Denzer D, Kubitzka RC, Ruzicka T, Schon MP. Critical role of neutrophils for the generation of psoriasiform skin lesions in flaky skin mice. *The Journal of investigative dermatology.* 2000;114(5):976–83. [PubMed: 10771480]
39. Chan JR, Blumenschein W, Murphy E, Diveu C, Wiekowski M, Abbondanzo S, et al. IL-23 stimulates epidermal hyperplasia via TNF and IL-20R2-dependent mechanisms with implications for psoriasis pathogenesis. *J Exp Med.* 2006;203(12):2577–87. [PubMed: 17074928]
40. Gracey E, Hromadová D, Lim M, Qaiyum Z, Zeng M, Yao Y, et al. TYK2 inhibition reduces type 3 immunity and modifies disease progression in murine spondyloarthritis. *J Clin Invest.* 2020;130(4):1863–78. [PubMed: 32149730]
41. Matos TR, O'Malley JT, Lowry EL, Hamm D, Kirsch IR, Robins HS, et al. Clinically resolved psoriatic lesions contain psoriasis-specific IL-17-producing alphabeta T cell clones. *J Clin Invest.* 2017;127(11):4031–41. [PubMed: 28945199]
42. Dillen CA, Pinsker BL, Marusina AI, Merleev AA, Farber ON, Liu H, et al. Clonally expanded gammadelta T cells protect against *Staphylococcus aureus* skin reinfection. *J Clin Invest.* 2018;128(3):1026–42. [PubMed: 29400698]
43. Kallioliadis GD, Zhao B, Triantafyllopoulou A, Park-Min K-H, Ivashkiv LB. Interleukin-27 inhibits human osteoclastogenesis by abrogating RANKL-mediated induction of nuclear factor of activated T cells c1 and suppressing proximal RANK signaling. *Arthritis Rheum.* 2010;62(2):402–13. [PubMed: 20112358]
44. Stumhofer JS, Laurence A, Wilson EH, Huang E, Tato CM, Johnson LM, et al. Interleukin 27 negatively regulates the development of interleukin 17-producing T helper cells during chronic inflammation of the central nervous system. *Nat Immunol.* 2006;7(9):937–45. [PubMed: 16906166]
45. Skeen MJ, Ziegler HK. Induction of murine peritoneal gamma/delta T cells and their role in resistance to bacterial infection. *J Exp Med.* 1993;178(3):971–84. [PubMed: 8350063]
46. Rei M, Goncalves-Sousa N, Lanca T, Thompson RG, Mensurado S, Balkwill FR, et al. Murine CD27(–) Vgamma6(+) gammadelta T cells producing IL-17A promote ovarian cancer growth via mobilization of protumor small peritoneal macrophages. *Proc Natl Acad Sci U S A.* 2014;111(34):E3562–70. [PubMed: 25114209]
47. Louis C, Souza-Fonseca-Guimaraes F, Yang Y, D'Silva D, Kratina T, Dagley L, et al. NK cell-derived GM-CSF potentiates inflammatory arthritis and is negatively regulated by CIS. *J Exp Med.* 2020;217(5).
48. Schett G, Lories RJ, D'Agostino M-A, Elewaut D, Kirkham B, Soriano ER, et al. Enthesitis: from pathophysiology to treatment. *Nat Rev Rheumatol.* 2017;13:731. [PubMed: 29158573]
49. Sherlock JP, Joyce-Shaikh B, Turner SP, Chao C-C, Sathe M, Grein J, et al. IL-23 induces spondyloarthropathy by acting on ROR- γ t+ CD3+CD4–CD8– enthesal resident T cells. *Nat Med.* 2012;18:1069. [PubMed: 22772566]
50. Corthay A, Hansson A-S, Holmdahl R. T lymphocytes are not required for the spontaneous development of enthesal ossification leading to marginal ankylosis in the DBA/1 mouse. *Arthritis Rheum.* 2000;43(4):844–51. [PubMed: 10765929]
51. Haley EK, Matmusaev M, Hossain IN, Davin S, Martin TM, Ermann J. The impact of genetic background and sex on the phenotype of IL-23 induced murine spondyloarthritis. *PLoS One.* 2021;16(5):e0247149. [PubMed: 33983951]

52. Adamopoulos IE, Tessmer M, Chao CC, Adda S, Gorman D, Petro M, et al. IL-23 is critical for induction of arthritis, osteoclast formation, and maintenance of bone mass. *Journal of immunology*. 2011;187(2):951–9.

Author Manuscript

Author Manuscript

Author Manuscript

Author Manuscript

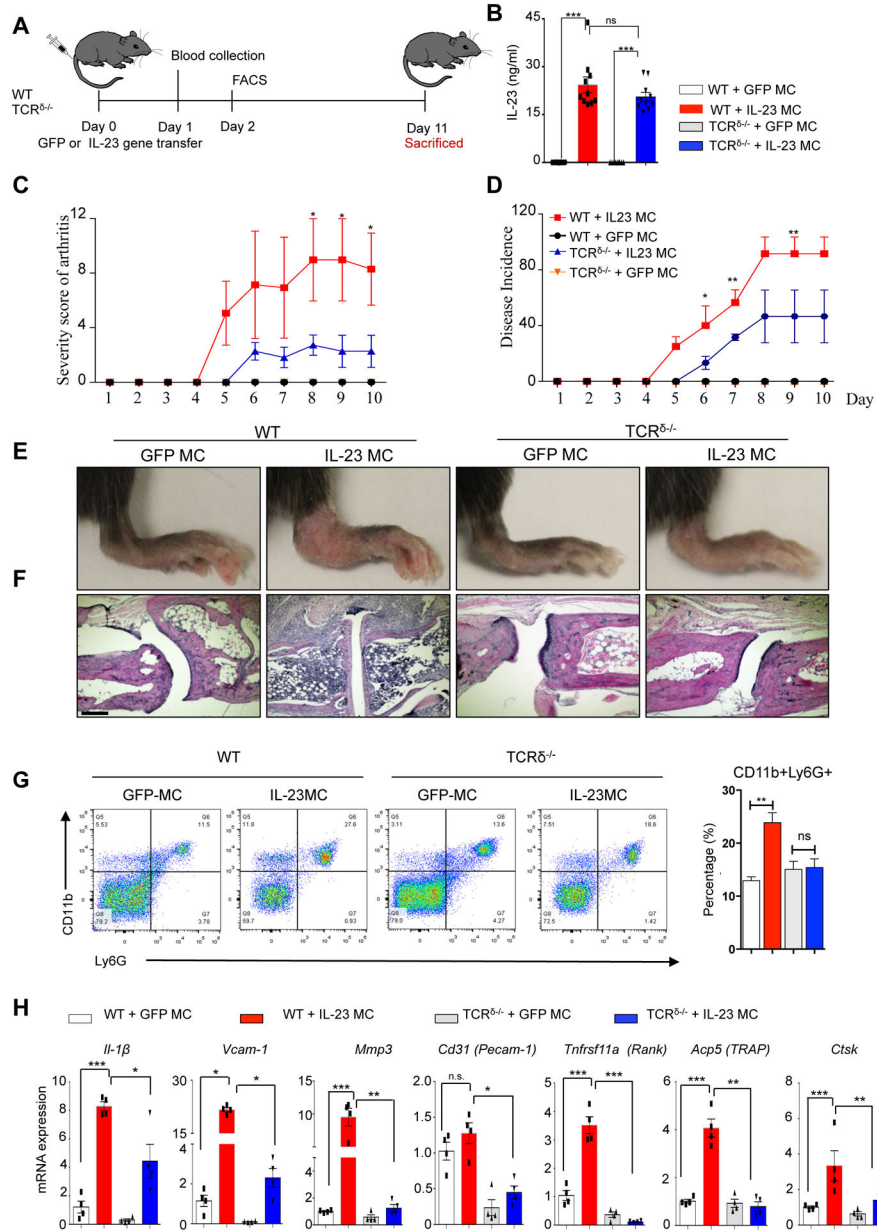


Figure 1: $\gamma\delta$ T cell deficiency ameliorates IL-23-induced joint inflammation. (A) Schematic of IL-23 and GFP (control) MC gene transfer model. (B) Serum IL-23 concentration 24 hours post IL-23 MC gene transfer. (C) Severity score of arthritis and (D) disease incidence in WT and $TCR^{\delta-/-}$ mice post IL-23 MC gene transfer. (Representative data of at three independent experiments 10–11 mice/group). (E) Photographs of murine ankles 11 days post IL-23 MC gene transfer showing inflamed mouse paws with extensive erythema and swelling of paws in IL-23 gene transfer mice compared to GFP MC and/or $TCR^{\delta-/-}$ mice. (F) H&E staining of murine ankle joints showing synovial inflammation with infiltrated cells. Scale bars, 200 μ m. (G) Representative flow cytometry dot plots gated on live lymphocytes of bone marrow 48 hours post IL-23 and/or GFP gene transfer in WT and $TCR^{\delta-/-}$ mice illustrating an increase in $CD11b^+Ly6G^+$ cell populations. (H) Gene

expression analysis of murine paws post IL-23 MC gene transfer showing an elevation of *Il1 β* , *Vcamp1*, *Mmp3*, *Pecamp1*, *Tnfrsf11a*, *Apc5*, and *Ctsk* compared to GFP MC (control) and/or TCR $\delta^{-/-}$ mice. Data represent mean \pm SEM of three independent experiments and 9–11 mice per each group. * $P < 0.05$; ** $P < 0.01$; *** $P < 0.001$ by Mann-Whitney test.

Author Manuscript

Author Manuscript

Author Manuscript

Author Manuscript

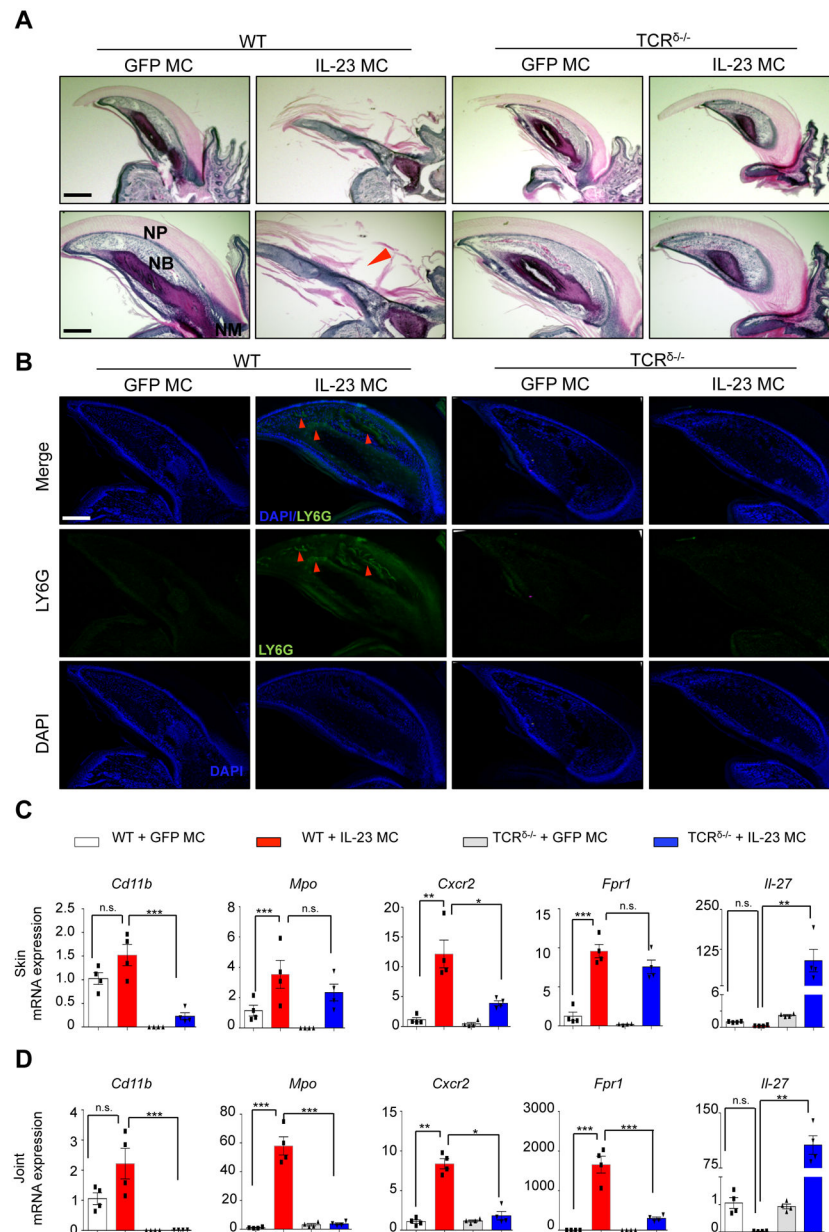


Figure 2: $\gamma\delta$ T cell deficiency prevents nail psoriasis and onycholysis by inhibiting neutrophil accumulation.

(A) H&E staining of murine nails showing nail psoriasis and onycholysis with infiltrated cells in nail bed (arrow). Scale bars, 300 μ m (upper) and 200 μ m (lower). Arrow indicates onycholysis. NP: nail plate; NB: nail bed. (B) Immunofluorescence images of Ly6G⁺ cells in nail post IL-23 MC gene transfer showing the neutrophil accumulation (arrows) in nail beds. Images are representative of 3 independent experiments, 10 mice per group. Scale bars, 200 μ m. (C) Gene expression analysis of neutrophil markers showing an elevation of *Cd11b*, *Mpo*, *Cxcr2*, *Fpr1* and *Il-27* in the skin and (D) joint tissues of IL-23 MC gene transfer WT mice and/or TCR^{δ-/-} mice compared to GFP MC (control). Data represent mean \pm SEM of three independent experiments. **P*<0.05; ** *P*<0.01; *** *P*<0.001 by Mann-Whitney.

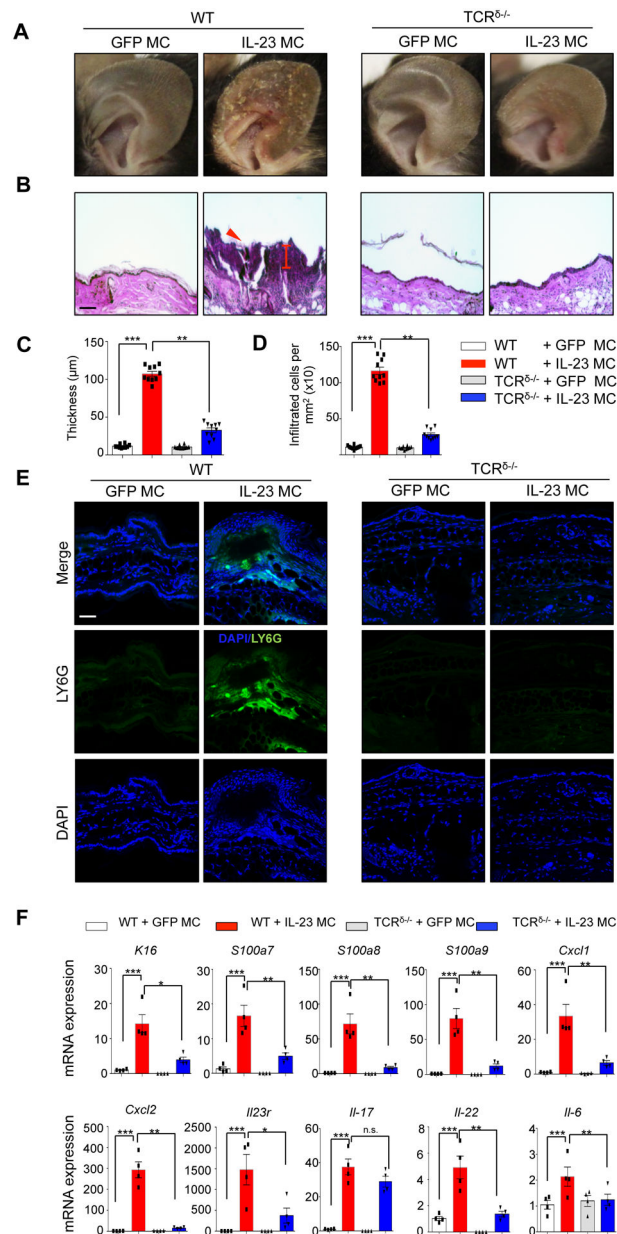


Figure 3: TCR^{δ-/-} deficiency suppresses IL-23 induced skin inflammation *in vivo*. (A) Photographs of murine ears 11 days post IL-23 MC gene transfer showing the development of silvery white scales in WT mice compared to GFP MC and/or TCR^{δ-/-} mice. (B) H&E staining of murine ears showing epidermal hyperplasia and number of infiltrated cells. Arrow indicates neutrophil exudates (Munro’s microabscess). (Images are representative of three independent experiments and 9–11 mice per each group. Scale bars, 100 µm). (C) Quantification of epidermal thickness (µm) and (D) infiltrated cell number. (E) Immunofluorescence images of Ly6G⁺ cells in ear post IL-23 MC gene transfer showing the neutrophil accumulation in dermis and epidermis. (F) Gene expression analysis of inflammatory markers showing an elevation of *K16*, *S100a7*, *S100a8*, *S100a9*, *Cxcl1*, *Cxcl2*, *Il23r*, *Il17a*, *Il22*, and *Il6* in the ears of IL-23 MC gene transfer WT mice compared to

GFP MC (control) and/or TCR^{δ-/-} mice. Data represent mean ± SEM of three independent experiments. * $P < 0.05$; ** $P < 0.01$; *** $P < 0.001$ by Mann-Whitney.

Author Manuscript

Author Manuscript

Author Manuscript

Author Manuscript

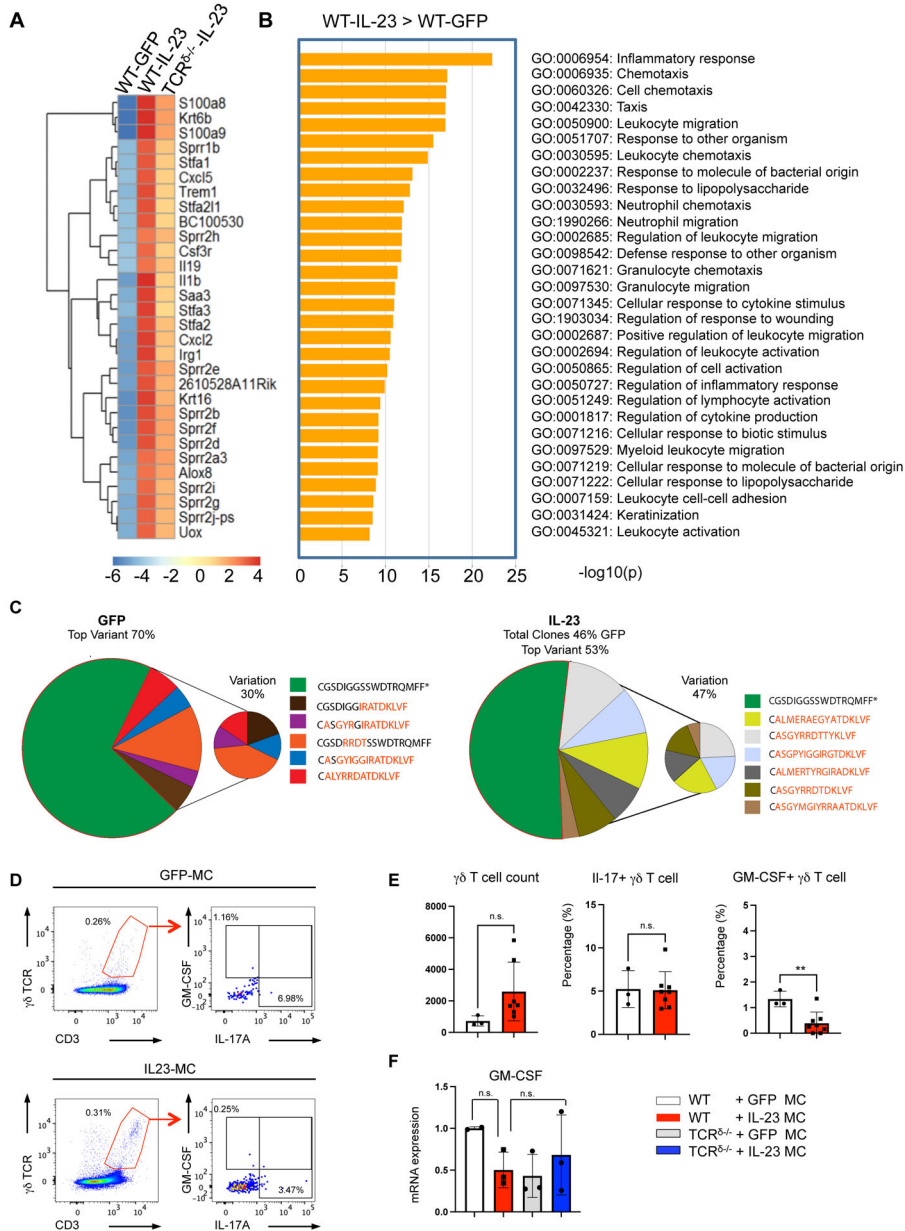


Figure 4. IL-23-induced skin inflammation is not associated with expansion of dermal $\gamma\delta$ T cells. Expression profiling of ear tissue collected from WT and TCR $\delta^{-/-}$ mice post GFP and/or IL-23 gene transfer, showing (A) Hierarchical clustering heatmap plot of top 30 differentially expressed genes (DEG) and (B) GO enrichment analysis for the upregulated genes post GFP and/or IL-23 gene transfer. (C) TCR repertoire analysis, depict in pie charts the distribution of TRD CDR3 in each treatment group cluster, different colors represent different TRD CDR3 sequences. The relative abundance of each TRD CDR3 sequence within each group is shown as percentage (%) beside the charts. (Representative data of at three independent experiments 3 mice per group). (D) Representative flow cytometry dot plots pre-gated on live lymphocytes and (E) bar graphs showing the gating strategy and percentage of CD3 $^{+}$ $\gamma\delta$ TCR $^{+}$ GM-CSF $^{+}$ IL-17A $^{+}$ cells in the skin of WT mice after 11 days

post IL-23 and/or GFP gene transfer. All data are shown as mean \pm SEM as determined by unpaired student's t-test. *P<0.05; ** P<0.01; *** P<0.001, ns = not significant. (F) GM-CSF mRNA expression in ears isolated from WT and/or TCR $\delta^{-/-}$ mice 11 days post GFP and/or IL-23 MC gene transfer.

Author Manuscript

Author Manuscript

Author Manuscript

Author Manuscript

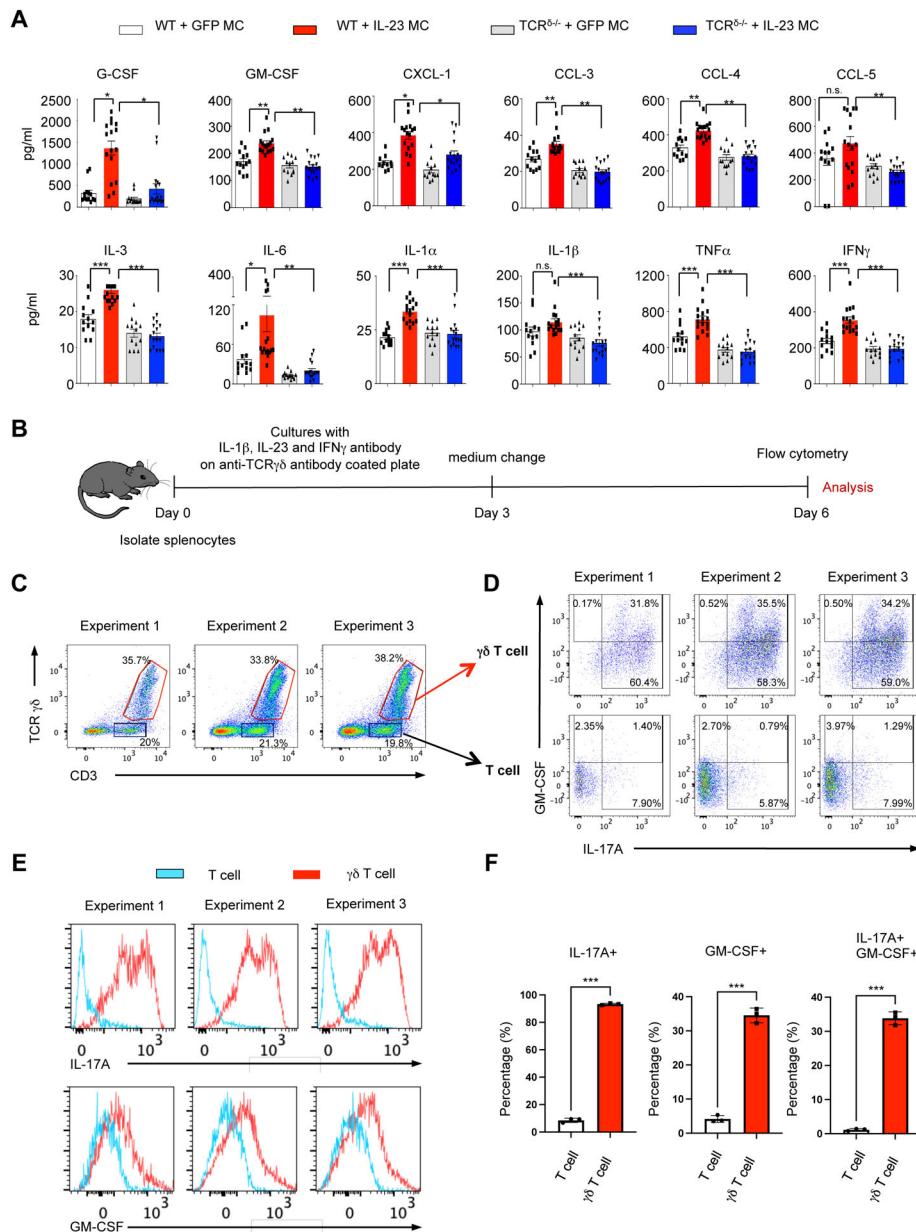


Figure 5. IL-23 induces the development of IL-17A⁺/GM-CSF⁺ $\gamma\delta$ T cells *in vitro*. (A) Serum cytokine and chemokine profile of WT mice and/or TCR $\delta^{-/-}$ mice post GFP and/or IL-23 MC gene transfer. Dotted line shows sensitivity of each assay. Data represent mean \pm SEM of three independent experiments. * P <0.05; ** P <0.01; *** P <0.001 by Mann-Whitney. (B) Schematic of $\gamma\delta$ T cell culture in WT mice. (C-D) Flow cytometry dot plots pre-gated on live lymphocytes showing the gating strategy, (E) histogram of IL-17A and GM-CSF, and (F) Bar plot showing percentage of IL-17A and GM-CSF positivity among the cultured T cell and $\gamma\delta$ T cells. All data are shown as mean \pm SEM as determined by unpaired student's t-test. * P <0.05; ** P <0.01; *** P <0.001, ns = not significant.